



Published in final edited form as:

*J Magn Reson Imaging*. 2018 June ; 47(6): 1459–1474. doi:10.1002/jmri.26027.

## LI-RADS 2017: An Update

Ania Z. Kielar, MD, FRCPC<sup>1,\*</sup>, Victoria Chernyak, MD, MS<sup>2</sup>, Mustafa R. Bashir, MD<sup>3</sup>, Richard K. Do, MD, PhD<sup>4</sup>, Kathryn J. Fowler, MD<sup>5</sup>, Donald G. Mitchell, MD, FACR<sup>6</sup>, Milena Cerny, MD<sup>7</sup>, Khaled M. Elsayes, MD, PhD<sup>8</sup>, Cynthia Santillan, MD<sup>9</sup>, Aya Kamaya, MD<sup>10</sup>, Yuko Kono, MD<sup>11</sup>, Claude B. Sirlin, MD<sup>9</sup>, An Tang, MD, Msc, FRCPC<sup>7</sup>

<sup>1</sup>Royal Victoria Regional Health Center, Barrie, Ontario, University of Ottawa, Ottawa Hospital Research Institute, Ottawa, Canada;

<sup>2</sup>Department of Radiology, Montefiore Medical Center, Bronx, New York, USA;

<sup>3</sup>Department of Radiology, Duke University Medical Center, Durham, North Carolina, USA, Center for Advanced Magnetic Resonance Development, Duke University Medical Center, Durham, North Carolina, USA, Department of Radiology, Memorial Sloan Kettering Cancer Center, New York, New York, USA;

<sup>4</sup>Department of Radiology, Memorial Sloan Kettering Cancer Center, New York, New York, USA;

<sup>5</sup>Department of Radiology, Washington University School of Medicine, St. Louis, Missouri, USA;

<sup>6</sup>Department of Radiology, Thomas Jefferson University, Philadelphia, Pennsylvania, USA;

<sup>7</sup>Department of Radiology, Centre Hospitalier de l'Université de Montréal (CHUM), Montréal, Québec, Canada;

<sup>8</sup>Department of Radiology, MD Anderson Cancer Center, Houston, Texas, USA;

<sup>9</sup>Department of Radiology, University of California, San Diego, California, USA;

<sup>10</sup>Department of Radiology, Stanford University, Palo Alto, California, USA;

<sup>11</sup>Department of gastroenterology, University of California, San Diego, California, USA

### Abstract

The computed tomography / magnetic resonance imaging (CT/MRI) Liver Imaging Reporting & Data System (LI-RADS) is a standardized system for diagnostic imaging terminology, technique, interpretation, and reporting in patients with or at risk for developing hepatocellular carcinoma (HCC). Using diagnostic algorithms and tables, the system assigns to liver observations category codes reflecting the relative probability of HCC or other malignancies. This review article provides an overview of the 2017 version of CT/MRI LI-RADS with a focus on MRI. The main LI-RADS categories and their application will be described. Changes and updates introduced in this version of LI-RADS will be highlighted, including modifications to the diagnostic algorithm and to the optional application of ancillary features. Comparisons to other major diagnostic systems for HCC will be made, emphasizing key similarities, differences, strengths, and

\*Address reprint requests to: A.K., Royal Victoria Regional Health Centre, 501 Georgian Drive, Barrie, ON L4M 6M2, Canada. aniakielar@gmail.com.

limitations. In addition, this review presents the new Treatment Response algorithm, while introducing the concepts of MRI nonviability and viability. Finally, planned future directions for LI-RADS will be outlined.

Hepatocellular carcinoma (HCC) is the second leading cause of cancer-related deaths worldwide<sup>1</sup> and the fastest-growing cause of cancer death in the United States and other Western nations. Cirrhosis—the endstage of chronic liver disease resulting from repetitive liver injury with cumulative liver damage—is the most important risk factor for HCC, especially in the Western world. While cirrhosis has many etiologies, the most common causes in North America and Europe are chronic hepatitis C virus (HCV), excess alcohol consumption, and nonalcoholic steatohepatitis (NASH). Worldwide, chronic infection by hepatitis B virus (HBV) is the single most important cause of cirrhosis and HCC—and this virus even predisposes to HCC formation prior to the development of cirrhosis due to its direct oncogenic effects<sup>1</sup>—but HBV is less common in Western nations.

One of the few malignancies that can be confidently diagnosed by imaging alone, HCC does not require biopsy confirmation when the imaging appearances are characteristic in patients with cirrhosis.<sup>2–4</sup> The ability to diagnose HCC by imaging alone places critical responsibility on radiologists. Use of a standardized reporting system, such as the computed tomography / magnetic resonance imaging (CT/MRI) Liver Reporting & Data System (LI-RADS), can help radiologists achieve the needed specificity, while also ensuring consistent reporting and communication between radiologists and other physicians within an institution, between different institutions, and worldwide. Importantly, the LI-RADS criteria were developed to diagnose with high specificity progressed HCCs, namely, HCCs that have advanced along the hepatocarcinogenesis pathway to the point where they are overtly malignant, with potential for vascular invasion and metastasis. Such HCCs characteristically are larger than 10 mm and manifest arterial phase hyperenhancement (APHE) in combination with other major features such as washout and/or capsule appearance. So-called early HCCs are precursors to progressed HCC and do not have the ability to invade vessels or metastasize. These are usually not diagnosable as HCC by LI-RADS, as they tend to lack APHE and one or more of the other major features required for confident HCC diagnosis.

This review article highlights version 2017 of LI-RADS, particularly as it pertains to the use of MRI for diagnosis and treatment response assessment. The main LI-RADS categories and their application will be described. Changes and updates introduced in this version of LI-RADS will be highlighted, including modifications to the diagnostic algorithm and to the optional application of ancillary features. Comparisons to other major diagnostic systems for HCC will be made, emphasizing key similarities, differences, strengths, and limitations. In addition, this review presents the new Treatment Response algorithm, while introducing the concepts of MRI nonviability and viability. Finally, planned future directions for LI-RADS will be outlined.

## LI-RADS: Overview

### Background

Conceived initially at two institutions in 2006, LI-RADS was further developed by an American College of Radiology (ACR)-endorsed committee convened in 2008 in a collaborative, multidisciplinary effort between diagnostic radiologists, hepatologists, interventional radiologists, and liver transplant surgeons. The goal of this group was to improve the consistency of communication between radiologists and requesting physicians.<sup>5</sup> The first iteration of LI-RADS was published in 2011, with major updates released in 2013, 2014, and 2017.

In order to maintain high specificity of the diagnostic algorithm, LI-RADS is applicable only in a population at high risk for developing HCC: this includes patients with known cirrhosis, chronic hepatitis B viral infection, current or prior HCC, including patients who have undergone liver transplantation for HCC. However, LI-RADS does not apply to patients who have cirrhosis as a result of congenital hepatic fibrosis, vascular disorders (including hereditary hemorrhagic telangiectasia, Budd-Chiari syndrome, chronic portal vein occlusion, and cardiac congestion), nor does it apply to patients with diffuse nodular regenerative hyperplasia. This is due to the predisposition of these particular conditions to development of vascular or regenerative nodules, which have imaging appearances overlapping with those of HCC.<sup>6</sup>

### Categories

LI-RADS allows discrete categorization of observations recognized at cross-sectional imaging including CT and MRI, with introduction of a separate algorithm for contrast-enhanced ultrasound (CEUS) in v2017.<sup>7</sup> The LI-RADS CT/MRI diagnostic algorithm includes categories ranging from 1 to 5, corresponding to LR-1 (definitely benign), LR-2 (probably benign), LR-3 (intermediate probability of malignancy), LR-4 (probably HCC), and LR-5 (definitely HCC)<sup>7</sup> (Fig. 1). The algorithm also includes an LR-M category for observations thought to be probably or definitely malignant but without features specific for HCC.

### Major Imaging Features

Major features for diagnosing HCC include:

- a. Nonrim arterial phase enhancement (APHE);
- b. Size;
- c. Nonperipheral washout appearance (“washout”) on the portal venous phase (PVP) or delayed phase (DP);
- d. An enhancing capsule appearance (“capsule”); and
- e. Threshold growth (TG).

The LI-RADS diagnostic table uses combinations of the major imaging features to arrive at the initial categories (Fig. 1), which can be then adjusted, based on the presence of ancillary features (AFs) (Table 1, Fig. 2).

The current criteria for LR-5 category include presence of nonrim APHE and one of following (Fig. 1):

- 10–19 mm with 2 additional major features;
- 10–19 mm with “washout” and visibility at antecedent US but with no “capsule” or threshold growth (LR-5us);
- 10–19 mm with 50% size increase in 6 months but with no “washout” or “capsule” (LR-5g);
- 20 mm with 1 additional major feature.

The criteria for LR-5 category has a positive predictive value approaching 100% among patients at risk for developing HCC.<sup>8,9</sup> Although the LI-RADS algorithm is equally applicable to both multiphase contrast-enhanced CT and MRI, Burrel et al showed that sensitivity of MRI was superior to CT for detecting HCC.<sup>10</sup> However, as with CT, sensitivity of MRI for detection of HCC decreases with smaller observations. In Burrel et al’s study, MRI had a sensitivity of 100% for nodules >20 mm, 84% for nodules 10–20 mm, and only 32% for nodules <10 mm in diameter.<sup>10</sup>

### Application of Major Features

It is important to emphasize that APHE, which is best evaluated in the late arterial phase on CT or MRI, is a required feature for LR-5 categorization<sup>11</sup> (Fig. 3). APHE is defined by the presence of enhancement that is unequivocally greater than that of the background liver.<sup>12,13</sup> In v2017, the distinction is made between rim and nonrim APHE, depending on whether or not enhancement is primarily confined to the periphery of the observation.<sup>13</sup> For LR-5 categorization, nonrim APHE must be present. Nonperipheral “washout” is defined as a visually assessed temporal reduction in enhancement in whole or at least in part relative to composite liver tissue from earlier to later phase resulting in hypoenhancement (Fig. 4c).<sup>13</sup> “Washout” is assessed in the PVP or DP with the use of the gadolinium-based extracellular contrast agents (ECA) or gadobenate, and in the PVP only if gadoxetate disodium is used.<sup>13</sup> The restriction applied to the gadoxetate-enhanced MRIs is based on the fact that apparent hypointensity of an observation in the 3–5 minutes transitional phase (TP) may be due to relative hyperenhancement of the parenchyma rather than a true tumor washout. As the result, specificity of an HCC diagnosis may decrease slightly if transitional phase hypointensity were to be accepted as “washout.”<sup>14,15</sup> With regard to the assessment of “washout,” Liu et al confirmed that detection of this imaging feature depends on many factors, which can include a radiologist’s subjective visual assessment and level of experience, in addition to window and level settings.<sup>16</sup>

In a quantitative study of multiphase CT by Liu et al, the percentage attenuation ratio for assessment of “washout” was found to have excellent sensitivity, specificity, positive predictive value, and negative predictive value for HCC characterization. Those authors also

noted that there is very good correlation with radiologists' subjective assessments of "washout."<sup>16</sup> A corollary quantitative definition for "washout" is needed for multiphase MRI, but has not yet been developed.

In v2017 of LI-RADS, an enhancing "capsule" is defined as a smooth, uniform, and sharply outlined area of enhancement around an observation which is either thicker or more conspicuous than fibrotic tissue associated with chronic liver disease.<sup>13</sup> This capsule can be detected in the PVP or on more DPs<sup>17</sup> (Fig. 3b).

The term Tumor In Vein (TIV) was retained in v2017 of LI-RADS (Fig. 5), but its use was refined. In prior versions, TIV was applied to assign a category of LR-5V, indicating HCC with macrovascular invasion into a vein. Since TIV is not specific for HCC—it can occur with non-HCC malignancies—LI-RADS v2017 applies TIV to establish the diagnosis of a malignant neoplasm with macrovascular invasion and changed the name of the category from LR-5V to LR-TIV. The change in category name is intended to emphasize and clarify that the underlying tumor may be other than HCC. TIV worsens prognosis of patients with HCC and other hepatic malignancies, since its presence is associated with more aggressive disease, metastatic spread beyond the liver, impaired liver function, and a concomitant reduced tolerance to treatment: in North America, TIV is considered a relative contraindication for surgical resection for HCC and—except as an investigational protocol—an absolute contraindication for liver transplantation.<sup>18</sup>

Inclusion of threshold growth in the LI-RADS algorithm was based on biological plausibility, expert opinion, and a desire to maintain consistency with the Organ Procurement and Transplant Network (OPTN), as it recognizes "50% diameter increase in 6 months" to be a major feature in diagnosing HCC. As a corollary, the v2017 of LI-RADS indicates that threshold growth is defined as a size increase of a mass by a minimum of 5 mm AND:

- a. 50% increase in size in 6 months, or
- b. 100% increase in size in >6 months, or
- c. an observation that was previously not seen on CT or MRI, and now measures 10 mm in 24 months (since prior CT or MRI).

Of note, it is imperative to perform the measurements using the same postcontrast phase, imaging sequence, and plane (axial vs. coronal or sagittal) on serial exams.

A recent systematic review of the major features by Tang et al indicated that prospectively validated estimates of diagnostic accuracy of growth are currently lacking.<sup>17</sup> Nevertheless, the authors concluded that there is biologic plausibility as well as sufficient indirect evidence to surmise that growth is an important feature of malignancy, and thus growth helps to differentiate HCC from benign entities.<sup>17</sup> Growth does not differentiate HCC from non-HCC malignancies, however; thus, if an observation with threshold growth also shows any feature suggestive of non-HCC malignancy (as discussed below), the most appropriate category is usually LR-M (Fig. 4).

## Version 2017 LI-RADS

### What's new?

The 2017 version of LI-RADS includes several updates compared to its most immediate antecedent version published in 2014. These include introduction of an ultrasound screening algorithm and CEUS diagnostic algorithm.<sup>19</sup> Additionally, a new “tumor response evaluation” algorithm was introduced for use with CT or MRI in the follow-up of patients who have undergone various types of locoregional therapy for presumed or pathologically proven HCC<sup>20</sup> (Fig. 6).

### Diagnostic Algorithm Update

The previously published CT/MRI LI-RADS categorization algorithm was updated for v2017, based on evaluation of published data since 2014. One major addition in v2017 is the definition of imaging features diagnostic of LR-M (probably or definitely malignant, although not HCC-specific) category. These include targetoid appearance on dynamic phases (rim APHE, peripheral “washout,” and delayed central enhancement), as well as targetoid appearance on diffusion, transitional phase, and hepatobiliary phase (Fig. 4).<sup>21</sup> The presence of any of the LR-M features is sufficient for LR-M categorization. In order to distinguish the LR-M features from the major features, v2017 added qualifiers “nonrim” and “nonperipheral” for APHE and “washout,” respectively<sup>13</sup> (Fig. 4).

### Ancillary Features

Ancillary features (AFs) are imaging findings that may be used to improve detection, increase confidence, or modify an observation category after the application of major features. These have been reported in the radiology literature and formalized in LI-RADS by grouping them in three classes: AFs favoring malignancy in general, AFs favoring HCC in particular, and AFs favoring benignity (Table 1). The use of AFs to refine the final category of an observation is unique to LI-RADS since other HCC diagnostic algorithms rely exclusively on the combination of the “major features” for HCC diagnosis.<sup>2,22,23</sup> While some AFs can be assessed on both CT and MRI imaging modalities (eg, subthreshold growth), many are specific to MRI, and some are specific to MRI with hepatobiliary agents.

### Changes to AF in LI-RADS v2017

Unlike previous versions of LI-RADS, the use of AFs was made optional. This was intended to encourage adoption of LI-RADS v2017, since there was concern that mandatory application of AFs could contribute to a perceived complexity of LI-RADS. Specific rules for adjusting the category with AFs have been explicitly defined to improve clarity (Fig. 2)<sup>24</sup>:

- AF that favor malignancy (including those that favor malignancy in general or HCC in particular) may be used to upgrade by one category up to LR-4. As with prior versions of LI-RADS, AFs cannot be used to upgrade the category to LR-5; this constraint is intended to preserve high specificity (ie, conceptually at 100%) of the LR-5 category.<sup>24</sup> Of note, the absence of any AF favoring malignancy

cannot be used to downgrade the category, because the absence of AFs favoring malignancy does not indicate benignity.

- AFs that favor benignity may be used to downgrade by one category. Similarly, the absence of these AFs cannot be used to upgrade the category.
- In the case of conflicting AFs (ie, one or more favoring malignancy and one or more favoring benignity), the final chosen category based on the major features should not be adjusted.

In addition to making AFs optional in LI-RADS v2017, two other modifications have been made to AFs. First, a new AF favoring malignancy known as “ultrasound visibility” was introduced. Second, an AF previously known as “distinctive rim” has been renamed “nonenhancing capsule.” These changes are discussed in further detail below.

Ultrasound visibility as an AF is defined as visibility on a previous US as a discrete nodule corresponding to the observation being evaluated on CT or MRI. In a patient at risk for HCC, the detection of a distinctive solid nodule or mass on US substantially elevates the likelihood of malignancy, hence the addition of this new AF.<sup>24</sup>

The modification to the term “nonenhancing capsule” in v2017 of LI-RADS was made to highlight the distinction between “enhancing capsule,” which is a major feature *indicative* of HCC, and “nonenhancing capsule,” which is an AF *suggestive* of HCC. An “enhancing capsule” is recognized by its smooth, uniform, sharp border around most or all of an observation, unequivocally thicker or more conspicuous than fibrotic tissue around background nodules, and visible as an enhancing rim in the portal venous phase, delayed phase, or transitional phase. In contrast, “nonenhancing capsule” describes a distinctive capsule-like appearance not manifesting as an enhancing rim in the post arterial extracellular phases.

Regarding mild-moderate increased signal intensity on T<sub>2</sub>-weighted images, which is considered an AF favoring malignancy in general, studies have shown that dysplastic nodules are almost never hyperintense on T<sub>2</sub>-weighted images.<sup>24</sup> Conversely, moderately or poorly differentiated HCC are associated with higher signal intensity on T<sub>2</sub>-weighted images: this signal intensity characteristic may be partly related to tumor vascularity and peliotic changes.<sup>24</sup> A study by Sofue et al, concluded that there is evidence for mild-moderate T<sub>2</sub> hyperintensity as an independent, significant, predictive risk factor of HCC (hazard ratio =1.84,  $P < 0.001$ ).<sup>25</sup> Granata et al found that in addition to major imaging features of LI-RADS, hyperintensity on T<sub>2</sub>-weighted images as well as restricted diffusion have a high positive predictive value for HCC.<sup>12</sup>

In LI-RADS v2017, restricted diffusion (high signal on diffusion-weighted imaging not attributable solely to T<sub>2</sub> shinethrough) is considered an AF of malignancy (although not specific to HCC). Ogihara et al confirmed the utility of diffusion-weighted imaging as an AF for HCC across a number of different vendors and b-values.<sup>26</sup> Another study by Shankar et al, noted a trend of decreasing ADC values in patients with HCC, correlated with increasing grade of the tumor.<sup>27</sup> This prospective study included patients single observations identified on screening ultrasounds, which were subsequently characterized with contrastenhanced



MRI (CE-MRI).<sup>27</sup> In these cases, the presence of restricted diffusion on DWI resulted in high sensitivity and specificity for HCC.<sup>27</sup>

Mosaic architecture refers to the presence within a single mass of multiple inner nodules and/or compartments of different intensities; this AF is specific for HCC, being very rare in other hepatic neoplasms.<sup>28</sup> Each inner nodule in a mosaic mass is thought to arise by clonal expansion from a distinct cell line with unique genetic and epigenetic alterations, sometimes manifesting different degrees of dedifferentiation in the hepatocarcinogenesis pathway. These biologically distinct inner nodules may be separated by fibrotic septa, hemorrhagic areas, and/or necrotic components. Mosaic architecture is more commonly seen in larger HCCs, greater than 3 cm in size<sup>29</sup> (Fig. 7).

Nodule-in-nodule is a subset of mosaic architecture where a single inner nodule with different imaging features is seen within a larger background nodule (Fig. 8). The inner nodule is thought to be a result of clonal expansion of cells more advanced along the hepatocarcinogenesis pathway compared to the outer nodule, and as a result, the inner nodule often has features of a progressed HCC (eg, APHE, “washout,” mild-moderate T<sub>2</sub> hyperintensity, and diffusion restriction), whereas the outer nodule usually has imaging features of a dysplastic nodule or early HCC (eg, absence of APHE, T<sub>1</sub> hyperintensity, T<sub>2</sub> iso- or hypointensity, and absence of diffusion restriction).<sup>24</sup>

Corona enhancement is defined as peri-observational enhancement in late AP or early PVP, where this enhancement is attributable to venous drainage from a tumor. It fades on later PVP and DP. This AF was further investigated by Goshima et al: In their study, the authors found that 75% of observations in patients at risk for HCC demonstrated this AF when a high-temporal, multiple hepatic arterial phase MRI protocol was used.<sup>30</sup> Depiction of corona enhancement on MRI will likely be more frequent as multiarterial acquisition techniques become commonplace.

Several other ancillary imaging findings have been associated with malignancy in general or HCC in particular, as outlined in Table 1 and demonstrated in Figs. 9–11, including iron sparing in a nodule (AF of malignancy, although not HCC in particular) (Fig. 9), iron within a nodule (AF favoring benignity) (Fig. 10), and blood product within a nodule (AF of malignancy, specific to HCC) (Fig. 11).

Given the growing body of evidence, AFs eventually may influence the decision between short-term imaging follow-up and/or biopsy of LI-RADS-4 observations. Some of the more specific AFs may one day also allow upgrading of LI-RADS category beyond LI-RADS-4.<sup>25</sup> The proportion of early or progressed HCC in the presence or absence of AFs will help inform their use in future versions of LI-RADS. As a result, the current rules of AF characterization and application to the LI-RADS algorithm may be updated in future versions of LI-RADS as new evidence accrues.

## Contrast Agents Available for Use in MRI for Diagnosis of HCC

In North America, the most commonly used contrast agents for liver MRI are extracellular agents (ECAs), such as gadodiamide, gadopentetate, and gadoteridol,<sup>31</sup> which are excreted



almost exclusively through the kidneys. When ECAs are used the diagnosis and staging of HCC is based mainly on assessment of vascularity, and the most important hallmark appearance of HCC is the presence of nonrim APHE followed by “washout” of the tumor in the portal venous and/or delayed phases.<sup>32</sup>

Hepatobiliary contrast agents are also used to detect and diagnose HCC, especially in many parts of Europe and Asia, as well as select centers in North America. Gadoxetate disodium, the most commonly used hepatobiliary agent for this purpose, has about 50%/50% excretion through the biliary tree and kidneys. Uptake of this agent by functioning hepatocytes precedes excretion into bile. The paramagnetic properties of this contrast agent causes shortening of the longitudinal relaxation time ( $T_1$ ) of the liver and biliary tree, causing a sustained increased signal in the liver parenchyma that peaks ~20 minutes after the injection.<sup>33</sup> It has been shown that hepatocyte uptake of gadoxetate mainly occurs via the organic anion transporter polypeptides OATP1B1 and B3 located at the sinusoidal membrane. Biliary excretion occurs via the multidrug resistance-associated proteins MRP2 at the canalicular membrane.<sup>26</sup> In early as well as progressed HCC, OATP1B1/B3 expression is often either absent or reduced compared to background liver parenchyma, whereas MRP2 expression is often increased.<sup>30</sup> As a result, HCCs tend to be hypointense compared to the liver in the delayed/hepatobiliary phase. Infrequently, HCCs have a high expression of OATP and low expression of MRP2 or have high expression of OATP and MRP2; these lesions can appear isointense or even hyperintense to the surrounding liver parenchyma.<sup>26,34</sup>

Several studies have shown that MRI performed with hepatobiliary contrast agents provides higher sensitivity compared to dynamic contrast-enhanced CT for the detection of HCC, as well as liver métastases.<sup>34–36</sup> According to Suh et al,<sup>37</sup> a hypointense nodule in the hepatobiliary phase of gadoxetate-enhanced MRI that is nonhypervascular in the arterial phase should be regarded as intermediate risk, whereas one that is hypervascular in the arterial phase should be considered high risk (Fig. 12). In v2017 of LI-RADS, signal hypointensity in an observation on hepatobiliary phase imaging is considered an AF of malignancy (Table 1).<sup>7</sup> The rationale is that hepatobiliary phase hypointensity is characteristic not only of HCC but of any lesion with absent OATP expression, including non-HCC malignancies (eg, cholangiocarcinoma and metastases to the liver from an extrahepatic primary).

A controversial issue is transitional phase hypointensity: While HCC typically shows hypointensity in the transitional phase, this feature does not provide the same specificity for HCC as washout appearance, and a spectrum of lesions can show hypointensity in this phase including cholangiocarcinomas and hemangiomas. The reason is that hypointensity in the transitional phase may reflect OATP-mediated enhancement of background liver rather than “washout” of the observation. To avoid miscategorization of cholangiocarcinomas and hemangiomas as LR-5, LI-RADS conservatively advocates transitional phase hypointensity as an AF favoring malignancy but not as a major feature. To qualify as washout, hypointensity must be discernable in the portal venous phase using gadoxetate disodium.

## Comparison of LI-RADS to Other Reporting Systems for HCC

Currently, several systems exist worldwide for diagnosing HCC by imaging and for determining subsequent patient management. Such systems include those from the American Association for the Study of Liver Disease (AASLD), OPTN, European Society of Gastrointestinal and Abdominal Radiology (ESGAR), as well as the European Association for the Study of the Liver (EASL).<sup>38,39</sup> According to the National Comprehensive Cancer Network (NCCN),<sup>40</sup> as well as the guidelines of EASL and AASLD, the diagnosis of HCC should be based on the detection of hypervascularity in the arterial phase with washout in the portal venous or delayed phases.<sup>41</sup> v2017 of LI-RADS has made efforts to ensure congruity with AASLD in particular, as well as OPTN.<sup>42</sup> For example, observations <1 cm cannot be classified as LR-5, since lesions <1 cm will not qualify as HCC in these other classification systems.<sup>7</sup> Compared with other systems, LI-RADS addresses the entire spectrum of observations rather than providing a binary assessment of HCC vs. not HCC. Also, LI-RADS gives guidance on all identified observations, including pseudolesions noted on CT and MRI as well as lesions identified by screening or surveillance ultrasound. Finally, LI-RADS was created for use by all radiologists, rather than just by experts in the field or those working in transplant centers.

There is still some variation in Asian reporting systems compared with each other and with AASLD, OPTN, and LI-RADS, including screening recommendations as well as variation in treatment algorithms by the Japanese Society of Hepatology (JSH) and Asian Pacific Association for the Study of the Liver (APASL).<sup>43,44</sup> This includes lack of minimum lesion size definitions in JSH or APASL. The updated JSH diagnostic algorithm is also the only one that includes gadoxetate-enhanced MRI as a first-line surveillance and diagnostic tool for HCC.<sup>43</sup> In contrast to the JSH algorithm, hypointensity on the hepatobiliary phase imaging is not yet included in the guidelines of the AASLD, EASL, or APASL guidelines.<sup>38</sup> The LI-RADS algorithm is equally applicable to MRI both with ECA and gadoxetate, with the exception of the aforementioned “washout” assessment, which is restricted to the PVP with gadoxetate as opposed to the PVP and DP with ECA and gadobenate.<sup>11,13</sup>

Some of these differences in reporting guidelines, particularly in Eastern Asia, reflect clinically relevant differences in patient population, underlying etiologies of liver disease, and available treatment options.<sup>45</sup>

## Strengths of MRI for Diagnosis of HCC

A meta-analysis by Hanna et al demonstrated that when comparing MRI, CT, and CEUS for characterizing and diagnosing HCC, MRI with hepatobiliary agents was found to have the highest overall sensitivity and positive predictive value.<sup>46</sup> In addition, MRI allows evaluation of the AFs, which may aid in the final LI-RADS category. In fact, the majority of AFs favoring malignancy, both in general and HCC specifically, are MRI-based (Table 1). Despite this, it is worth noting that the major societies in North America, as well as LI-RADS, recommend either CT or MRI for characterization and categorization of liver observations.

Recent technical advances in MRI have led to increased temporal resolution in postcontrast imaging, including the ability to obtain images in the early, mid, and later arterial phase. Since the timing of the late arterial phase varies from patient to patient and depends on a number of factors, imaging the entire liver several times consecutively in a short period of time increases the likelihood of capturing the late arterial phase, which is the optimal imaging phase for assessing APHE in most HCCs.<sup>36</sup> Additionally, acquisition of multiple arterial phases allows improved recognition of transient phenomena such as corona enhancement, an AF of malignancy in general.<sup>24,30</sup> While promising, the clinical impact of performing high temporal resolution arterial phase imaging routinely needs to be further investigated.

Compared to CT, MRI has the added benefit of subtraction imaging, which can be helpful in situations where there is underlying high signal intensity material or hemorrhage within or around an observation on T<sub>1</sub>-weighted images.<sup>47</sup> Subtraction images are particularly useful following various types of locoregional therapies.<sup>47</sup>

## Potential Pitfalls of MRI in Patients With Cirrhosis

Many patients with cirrhosis may have concomitant medical conditions such as emphysema or heart disease, which may preclude them from being able to hold their breath for extended periods of time. Also, encephalopathy can decrease patient compliance with breath-holding. In addition, hemodynamic alterations in patients with cirrhosis can delay the arrival of contrast material to the liver at MRI (as well as at CT), leading to a mistiming of the late arterial phase, which is critical to assess for the presence of APHE.<sup>36</sup> Improvements in technology have led to the development of newer MRI sequences that can be done either with free breathing or with much shorter breath-holds than before; the increasing availability of such sequences is expected to reduce some of these technical limitations.

Ascites can contribute to the presence of severe artifact on MRI, including dielectric effects with resulting B<sub>1</sub> field heterogeneity and fluid motion artifacts (Fig. 13), thereby reducing image quality, especially on T<sub>2</sub>-weighted fast spin echo or single-shot fast spin echo sequences, and obscuring observations in or outside the liver. Drainage of ascites may be helpful in some cases to reduce these issues, although CT may be the imaging modality of choice in most patients with large-volume ascites.

Severe liver parenchymal dysfunction, particularly in advanced cirrhosis, can result in impaired hepatobiliary contrast agent uptake and therefore reduce its sensitivity in identifying areas of signal hypointensity expected in HCC. Further study is needed to determine the prevalence of this pitfall.<sup>48</sup>

Another growing concern for MRI is the potential for gadolinium deposition in tissue. Although nephrogenic systemic fibrosis can be avoided in patients with acute kidney injury and severe renal dysfunction by avoiding certain formulations of gadolinium-based contrast media and by using US Food and Drug Administration (FDA)-approved weight-adjusted doses, there is emerging concern regarding gadolinium deposition in the body, including the

brain, even in patients without renal dysfunction. Future potential effects are currently unknown and further investigations are needed.<sup>49</sup>

Finally, Burrel et al cautioned that special attention must be given to perfusion alterations, as these are commonly identified in cirrhotic liver and can be associated with false-positive reports.<sup>10</sup> Vascular shunts and other pseudolesions can impair diagnostic performance by mimicking HCCs (reducing specificity) or obscuring true HCC lesions (reducing sensitivity). Unlike HCC, vascular pseudolesions lack a mass-like appearance. As these shunts may occasionally show mild hypoenhancement on late dynamic or hepatobiliary phase images and mild hyperintensity on T<sub>2</sub>-weighted or diffusion-weighted images, leading to a diagnostic dilemma.<sup>23</sup> Recognizing the nonmass-like appearance is key. Fortunately, these pseudolesions do not have washout or capsule appearances, and so rarely would be categorized LR-5 even if they can cause some degree of diagnostic confusion.

## LI-RADS v2017 Treatment Response

### Treatment Response Algorithm

This new algorithm was introduced in v2017 of LI-RADS and is designed to help assess observations following locoregional therapy, using either dynamic CT or MRI (Fig. 6). Various types of locoregional therapies are available for HCC, such as thermal ablation (eg, radiofrequency ablation, microwave ablation), transcatheter therapies (with or without chemotherapeutic agents), as well as localized radiotherapy. Currently, this algorithm is not designed for systemic therapy or, unless the recurrence is at the surgical margin, in postoperative cases<sup>12</sup>

### Concept of Tumor Viability

The identification of “viable tumor” following one of these local treatments warrants further management and potentially affects transplantation eligibility (Fig. 14).<sup>25</sup>

Existing guidelines for assessing response in solid tumors (RECIST and modified RECIST) address patient-level assessments, but do not address the individual treated lesions following different locoregional therapies.<sup>7</sup> The new Treatment Response Algorithm addresses this gap and offers a single, comprehensive approach to assess treatment response for individual lesions after locoregional therapy.<sup>7</sup>

As described earlier, MRI has advantages for evaluation of presumed HCC treated with various types of locoregional therapy, since there is the possibility of performing subtraction imaging: Many therapies including radiofrequency ablation and microwave ablation lead to areas of hemorrhage in the ablation zone. After injection of a contrast agent either for CT or MRI, it can be a challenge to determine if there is enhancement or simply “shinethrough” of the intrinsic brightness of the treated lesion: By performing subtraction imaging on MRI, areas of residual disease can be identified more confidently.<sup>19</sup>

In patients undergoing transarterial chemoembolization (TACE), a hyperdense substance, iodized oil, is often injected at the time of the fluoroscopically guided procedure.<sup>26</sup> Iodized oil, based on poppy seed oil, can be used as a radio-opaque intra-arterially administered

contrast agent. Although accumulation of iodized oil on CT evaluation shortly after TACE portends a technically satisfactory result, it can be difficult to identify areas of residual hyperenhancement. Iodized oil is sometimes visible at MRI as a region of signal loss from T<sub>1</sub>-weighted in-phase to out-of-phase images, but this does not interfere with the assessment for residual viable tumor using this modality (Fig. 14).<sup>26</sup>

Further evolution and refinement of the LI-RADS Treatment Response Algorithm will be made in future iterations of LI-RADS as new literature is published regarding locoregional therapies, particularly in patients undergoing stereotactic body radiation therapy (SBRT) and yttrium-90 treatments, where evaluation can be challenging in the first several months due to radiation-induced changes that are physiologically very different from expected changes post thermal treatments.<sup>50</sup>

## Future Directions and Adoption

One of the long-term goals for LI-RADS is to promote the adoption of a single, unified imaging system for HCC diagnosis among diagnostic radiologists for clinical care, research, and education. The successful accomplishment of this vision would improve communication with clinicians, pathologists, and surgeons, improve consistency of radiology reports, and lead to the creation of large registries for more effective, large-scale research projects.

The evidence-based approach of LI-RADS is one of its major strengths, but the associated complexity is also a potential barrier for adoption. The complexity is partly explained by the overlapping appearances on CT and MRI between precursor lesions and frank HCC. Therefore, evaluation of patients at risk for developing HCC requires not only scales in the categorization of liver observations but robust follow-up and consistent, evidence-based management pathways. Future work in creating synoptic reporting templates that include standardized imaging features and automated LI-RADS category determination may play an important role in promoting broader acceptance of this system.

## Conclusion

MRI plays an essential role in imaging patients at risk for HCC and is an important tool when categorizing liver observations using v2017 of LI-RADS. One of the benefits of using MRI is the inclusion of multiple ancillary imaging features that may help characterize liver observations. However, to preserve congruency with other HCC diagnostic algorithms, the use of AFs, including delayed hepatobiliary phase hypointensity, remains optional. Future research is still needed to compare the diagnostic performance of MRI compared to CT, to define the importance of individual AF in diagnosing HCC and/or predicting its biological behavior and prognosis, and to define the role of hepatobiliary agents for MRI screening of patients at risk for HCC.

## Acknowledgments

We acknowledge the remaining v2017 LI-RADS writing group members and all remaining members of the LI-RADS steering committee. This includes: Matthew McInnes, MD, FRCPC, Jay P Heiken, MD, Amit Singal, MD, Adrija Mamidipalli, MD, Alessandro Furlan, MD, Alexander Towbin, MD, Amol Shah, MD, Andrej Lyshchik, MD, Avinash Kambadakone, MD, Demetri Papadatos, MD, FRCPC, Elizabeth Hecht, MD, Eric Ehman, MD, Evan

Siegelman, MD, Hero Hussain, MD, Cheng Hong, MD, Jonathan Hooker, MD, Jeffrey Weinreb, MD, Judy Wawira, MD, Rohit Loomba, MD, Marc Kohli, MD, Maxime Ronot, MD, Reena Jha, MD, Alexandra Roudenko, MD, Soudabeh Fazeli, MD, Tom Hope, MD. Grant Support: There was no specific grant support for this review article.

#### Conflict of Interest

Ania Kielar has a research grant from General Electric regarding MRI of the liver for hepatocellular carcinoma. An Tang is supported by a research scholarship from Fonds de Recherche du Québec-Santé and Fondation de l'Association des Radiologistes du Québec (FRQS-ARQ 34939). Mustafa Bashir reports research grants from Siemens Healthcare, GE Healthcare, NGM Biopharmaceuticals, TaiwanJ Pharma, and Madrigal Pharmaceuticals. Mustafa Bashir receives consulting fees from RadMD. Claude Sirlin reports research grants from GE and Siemens.

## References

1. Torre LA, Bray F, Siegel RL, et al. Global cancer statistics, 2012. *CA Cancer J Clin* 2015;65:87–108. [PubMed: 25651787]
2. Bruix J, Sherman M. Management of hepatocellular carcinoma: an update. *Hepatology* 2011;53:1020–1022. [PubMed: 21374666]
3. Chernyak V, Santilan CS, Papadatos D, Sirlin CB. LI-RADS((R)) algorithm: CT and MRI. *Abdom Radiol* 2018;43:111–126.
4. Tang A, Valasek MA, Sirlin CB. Update on the Liver Imaging Reporting and Data System: What the pathologist needs to know. *Adv Anat Pathol*. 2015;22:314–322. [PubMed: 26262514]
5. Sirlin CB. The LI-RADS adventure—a personal statement. *Abdom Radiol* 2018;43:1–2.
6. Tang A, Hallouch O, Chernyak V, Kamaya A, Sirlin CB. Epidemiology of hepatocellular carcinoma: target population for surveillance and diagnosis. *Abdom Radiol* 2018;43:13–25.
7. ACR Version 2017 LI-RADS Core version. Available from: [chrome-extension://oemmndcbldboiebfnladdacbfmadadm/https://www.acr.org/-/media/ACR/Files/RADS/LI-RADS/LIRADS\\_2017\\_Core.pdf?la=en](chrome-extension://oemmndcbldboiebfnladdacbfmadadm/https://www.acr.org/-/media/ACR/Files/RADS/LI-RADS/LIRADS_2017_Core.pdf?la=en). Accessed January 18, 2018.
8. Forner A, Vilana R, Ayuso C, et al. Diagnosis of hepatic nodules 20 mm or smaller in cirrhosis: Prospective validation of the noninvasive diagnostic criteria for hepatocellular carcinoma. *Hepatology* 2008;47: 97–104. [PubMed: 18069697]
9. Rimola J, Forner A, Tremosini S, et al. Non-invasive diagnosis of hepatocellular carcinoma <2cm in cirrhosis. Diagnostic accuracy assessing fat, capsule and signal intensity at dynamic MRI. *J Hepatol* 56:1317–1323.
10. Burrel M, Llovet JM, Ayuso C, et al. MRI angiography is superior to helical CT for detection of HCC prior to liver transplantation: an explant correlation. *Hepatology* 2003;38:1034–1042. [PubMed: 14512891]
11. Santil Ian C, Chernyak V, Sirlin C. LI-RADS categories: concepts, definitions, and criteria. *Abdom Radiol* 2018;43:101–110.
12. Granata V, Fusco R, Avallone A, et al. Critical analysis of the major and ancillary imaging features of LI-RADS on 127 proven HCCs evaluated with functional and morphological MRI: Lights and shadows. *Oncotarget* 2017;8:51224–51237. [PubMed: 28881643]
13. Santil Ian C, Fowler K, Kono Y, Chernyak V. LI-RADS major features: CT, MRI with extracellular agents, and MRI with hepatobiliary agents. *Abdom Radiol* 2018;43:75–81.
14. Joo I, Lee JM, Lee DH, Jeon JH, Han JK, Choi BI. Noninvasive diagnosis of hepatocellular carcinoma on gadoxetic acid-enhanced MRI: can hypointensity on the hepatobiliary phase be used as an alternative to washout? *Eur Radiol* 2015;25:2859–2868. [PubMed: 25773941]
15. Choi SH, Lee SS, Kim SY, et al. Intrahepatic cholangiocarcinoma in patients with cirrhosis: differentiation from hepatocellular carcinoma by using gadoxetic acid-enhanced MR imaging and dynamic CT. *Radiology* 2017;282:771–781. [PubMed: 27797675]
16. Yi Liu, Shin LK, Jeffrey RB, Kamaya A. Quantitatively Defining Washout in Hepatocellular Carcinoma. *Am J Roentgenol* 2013;200: 84–89.
17. Tang A, Bashir MR, Corwin MT, et al. Evidence supporting LI-RADS major features for CT- and MR imaging-based diagnosis of hepatocellular carcinoma: a systematic review. *Radiology* 2018;286: 29–48. [PubMed: 29166245]



18. Santillan C, Chernyak V, Sirlin C. LI-RADS categories: concepts, definitions, and criteria. *Abdom Radiol* 2018;43:101–110.
19. Kim TK, Noh SY, Wilson SR, et al. Contrast-enhanced ultrasound (CEUS) liver imaging reporting and data system (LI-RADS) 2017 — a review of important differences compared to the CT/MRI system. *Clin Mol Hepatol* 2017;23:280–289. [PubMed: 28911220]
20. Kielar A, Fowler KJ, Lewis S, et al. Locoregional therapies for hepatocellular carcinoma and the new LI-RADS treatment response algorithm. *Abdom Radiol* 2018;43:218–230.
21. Fowler KJ, Potretzke TA, Hope TA, Costa EA, Wilson SR. LI-RADS M (LR-M): definite or probable malignancy, not specific for hepatocellular carcinoma. *Abdom Radiol* 2018;43:149–157.
22. Wald C, Russo MW, Heimbach JK, Hussain HK, Pomfret EA, Bruix J. New OPTN/UNOS policy for liver transplant allocation: standardization of liver imaging, diagnosis, classification, and reporting of hepatocellular carcinoma. *Radiology* 2013;266:376–382. [PubMed: 23362092]
23. EASL-EORTC clinical practice guidelines: management of hepatocellular carcinoma. *J Hepatol* 2012;56:908–943. [PubMed: 22424438]
24. Chernyak V, Tang A, Flusberg M, et al. LI-RADS((R)) ancillary features on CT and MRI. *Abdom Radiol* 2018 Jan;43:82–100.
25. Sofue K, Burke LMB, Nilmini V, et al. Liver imaging reporting and data system category 4 observations in MRI: Risk factors predicting upgrade to category 5. *J Magn Reson Imaging* 2017;46: 783–792. [PubMed: 28083902]
26. Ogiwara Y, Kitazume Y, Iwasa Y, et al. Prediction of histological grade of hepatocellular carcinoma using quantitative diffusion-weighted magnetic resonance imaging: a retrospective multi-vendor study. *Br J Radiol* 2017;20170728.
27. hankar S, Kaira N, Bhatia A, et al. Role of diffusion weighted imaging (DWI) for hepatocellular carcinoma (HCC) detection and its grading on 3T MRI: A prospective study. *J Clin Exp Hepatol* 2016;6:303–310. [PubMed: 28003720]
28. Choi BI, Lee GK, Kim ST, Han MC. Mosaic pattern of encapsulated hepatocellular carcinoma: correlation of magnetic resonance imaging and pathology. *Gastrointest Radiol* 1990;15:238–240. [PubMed: 2160392]
29. Yoshida T, Matsue H, Okazaki N, Yoshino M. Ultrasonographic differentiation of hepatocellular carcinoma from metastatic liver cancer. *J Clin Ultrasound* 1987;15:431–437. [PubMed: 2839556]
30. Goshima S, Noda Y, Kajita K, et al. Gadoteric acid-enhanced high temporal-resolution hepatic arterial-phase imaging with view-sharing technique: Impact on the LI-RADS category. *Eur J Radiol* 2017;94: 167–173. [PubMed: 28709718]
31. Mitsumori LM, Bhargava P, Essig M, Maki JH. Magnetic resonance imaging using gadolinium-based contrast agents. *Top Magn Reson Imaging* 2014;23:51–69.
32. Sangiovanni A, Manini MA, Iavarone M, et al. The diagnostic and economic impact of contrast imaging techniques in the diagnosis of small hepatocellular carcinoma in cirrhosis. *Gut* 2010;59:638–644. [PubMed: 19951909]
33. Seale MK, Catalano OA, Saini S, Hahn PF, Sahani DV. Hepatobiliary-specific MR contrast agents: role in imaging the liver and biliary tree. *RadioGraphics* 2009;29:1725–1748. [PubMed: 19959518]
34. Van Beers BE, Pastor CM, Hussain HK. Primovist, Eovist: What to expect? *J Hepatol* 2012;57:421–429. [PubMed: 22504332]
35. Chen L, Zhang L, Bao J, et al. Comparison of MRI with liver-specific contrast agents and multidetector row CT for the detection of hepatocellular carcinoma: a meta-analysis of 15 direct comparative studies. *Gut* 2013;62:1520–1521. [PubMed: 23929696]
36. Niendorf E, Spilseth B, Wang X, Taylor A. Contrast enhanced MRI in the diagnosis of HCC. *Diagnostics* 2015;5:383–398. [PubMed: 26854161]
37. Suh CH, Kim KW, Pyo J, Lee J, Kim SY, Park SH. Hypervascular transformation of hypovascular hypointense nodules in the hepatobiliary phase of gadoteric acid-enhanced MRI: A systematic review and meta-analysis. *AJR Am J Roentgenol* 2017;209:781–789. [PubMed: 28742376]
38. Aube C, Oberti F, Lonjon J, et al. EASL and AASLD recommendations for the diagnosis of HCC to the test of daily practice. *Liver Int* 2017; 37:1515–1525. [PubMed: 28346737]



39. Neri E, Bali MA, Ba-Ssalamah A, et al. ESGAR consensus statement on liver MR imaging and clinical use of liver-specific contrast agents. *Eur Radiol* 2016;26:921–931. [PubMed: 26194455]
40. Benson AB 3rd, D'Angelica MI, et al. NCCN Guidelines Insights: Hepatobiliary Cancers, Version 1.2017. *J Natl Compreh Cancer Network* 2017;15:563–573.
41. EASL-EORTC clinical practice guidelines: management of hepatocellular carcinoma. *Eur J Cancer* 2012;48:599–641. [PubMed: 22424278]
42. Wald C, Russo MW, Heimbach JK, Hussain HK, Pomfret EA, Bruix J. New OPTN/UNOS policy for liver transplant allocation: standardization of liver imaging, diagnosis, classification, and reporting of hepatocellular carcinoma. *Radiology* 2013;266:376–382. [PubMed: 23362092]
43. Omata M, Cheng A-L, Kokudo N, et al. Asia-Pacific clinical practice guidelines on the management of hepatocellular carcinoma: a 2017 update. *Hepatol Int* 2017;11:317–370. [PubMed: 28620797]
44. Renzulli M, Golfieri R. Proposal of a new diagnostic algorithm for hepatocellular carcinoma based on the Japanese guidelines but adapted to the Western world for patients under surveillance for chronic liver disease. *J Gastroenterol Hepatol* 2016;31:69–80. [PubMed: 26312574]
45. Mokdad AA, Lopez AD, Shahrz S, et al. Liver cirrhosis mortality in 187 countries between 1980 and 2010: a systematic analysis. *BMC Med* 2014; 12:145. [PubMed: 25242656]
46. Hanna RF, Miloushev VZ, Tang A, et al. Comparative 13-year meta analysis of the sensitivity and positive predictive value of ultrasound, CT, and MRI for detecting hepatocellular carcinoma. *Abdom Radiol* 2016;41:71–90.
47. Sainani NI, Gervais DA, Mueller PR, Arellano RS. Imaging after percutaneous radiofrequency ablation of hepatic tumors. Part 2. Abnormal findings. *Am J Roentgenol* 2013;200:194–204. [PubMed: 23255762]
48. Kim SH, Kim SH, Lee J, et al. Gadoxetic acid-enhanced MRI versus triple-phase MDCT for the preoperative detection of hepatocellular carcinoma. *Am J Roentgenol* 2009;192:1675–1681. [PubMed: 19457834]
49. Gulani V, Calamante F, Shellock FG, Kanal E, Reeder SB. Gadolinium deposition in the brain: summary of evidence and recommendations. *Lancet Neurol* 2017;16:564–570. [PubMed: 28653648]
50. Geschwind J-FH. Locoregional therapy for patients with hepatocellular carcinoma. *Gastroenterol Hepatol* 2015;11:698–700.

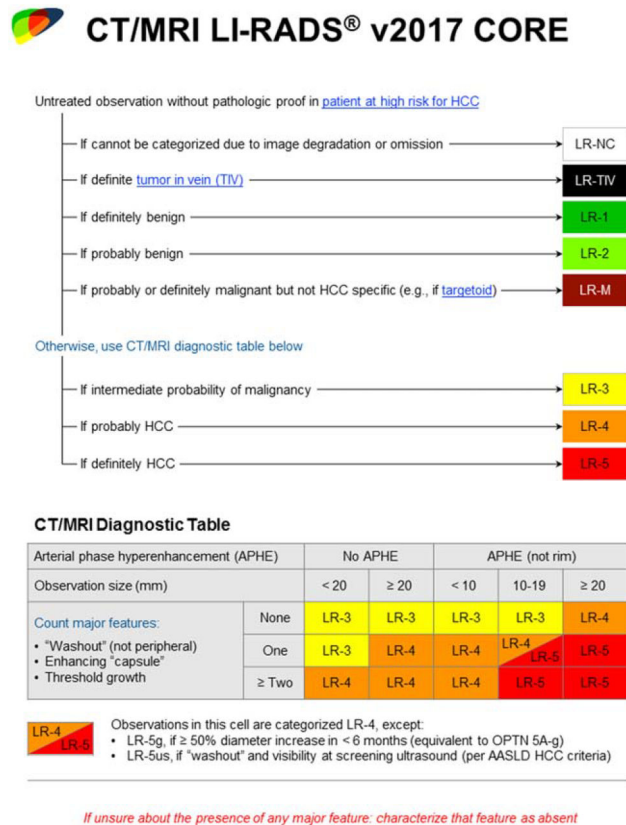


**FIGURE 1:**  
v2017 LI-RADS CT/MRI algorithm for categorizing liver observations identified in patients  
"at risk" for HCC. Reprinted with permission from the American College of Radiology.

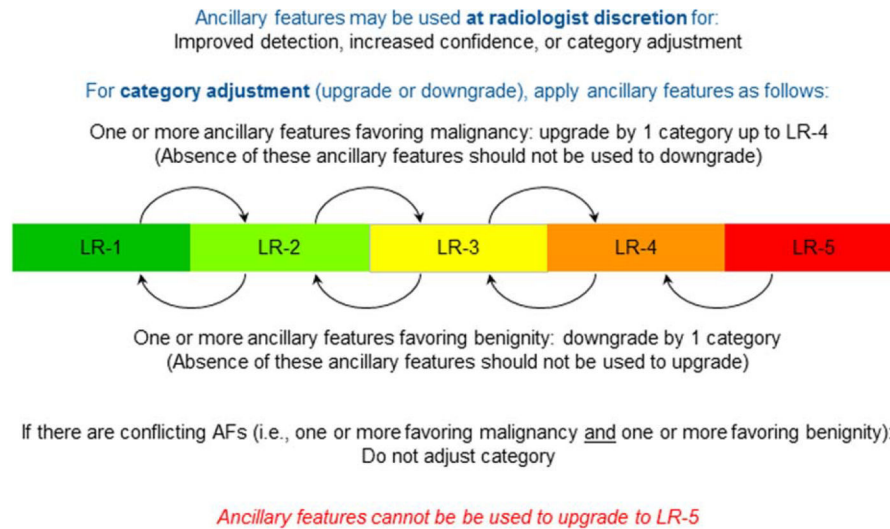


**FIGURE 2:**  
v2017 LI-RADS demonstrating integration of ancillary features and their effect on the final LI-RADS categorization. Note: Use of ancillary features is considered optional in v2017.  
Reprinted with permission from the American College of Radiology.

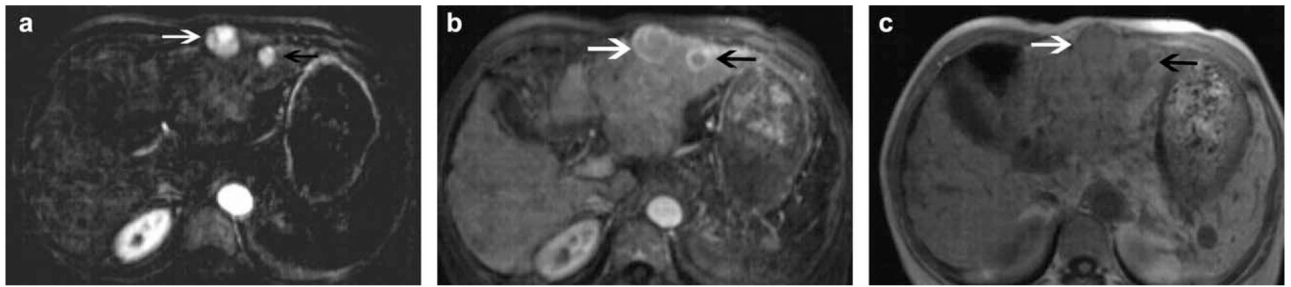


**FIGURE 3:**

Two observations identified in a 52-year-woman with ethanol-induced liver cirrhosis. The larger observation measures 22 mm (white arrow) and the smaller measures 9 mm (black arrow). Both demonstrate arterial enhancement (a), with washout and peripheral capsule on portal venous phase (b), there is low signal intensity on T<sub>1</sub>-weighted images, in-phase (c). Given the imaging findings, the larger observation is categorized as LI-RADS-5 and the smaller, due to being <1 cm in maximum diameter, is categorized as LI-RADS-4: this rule was created in order to be consistent with OPTN criteria.

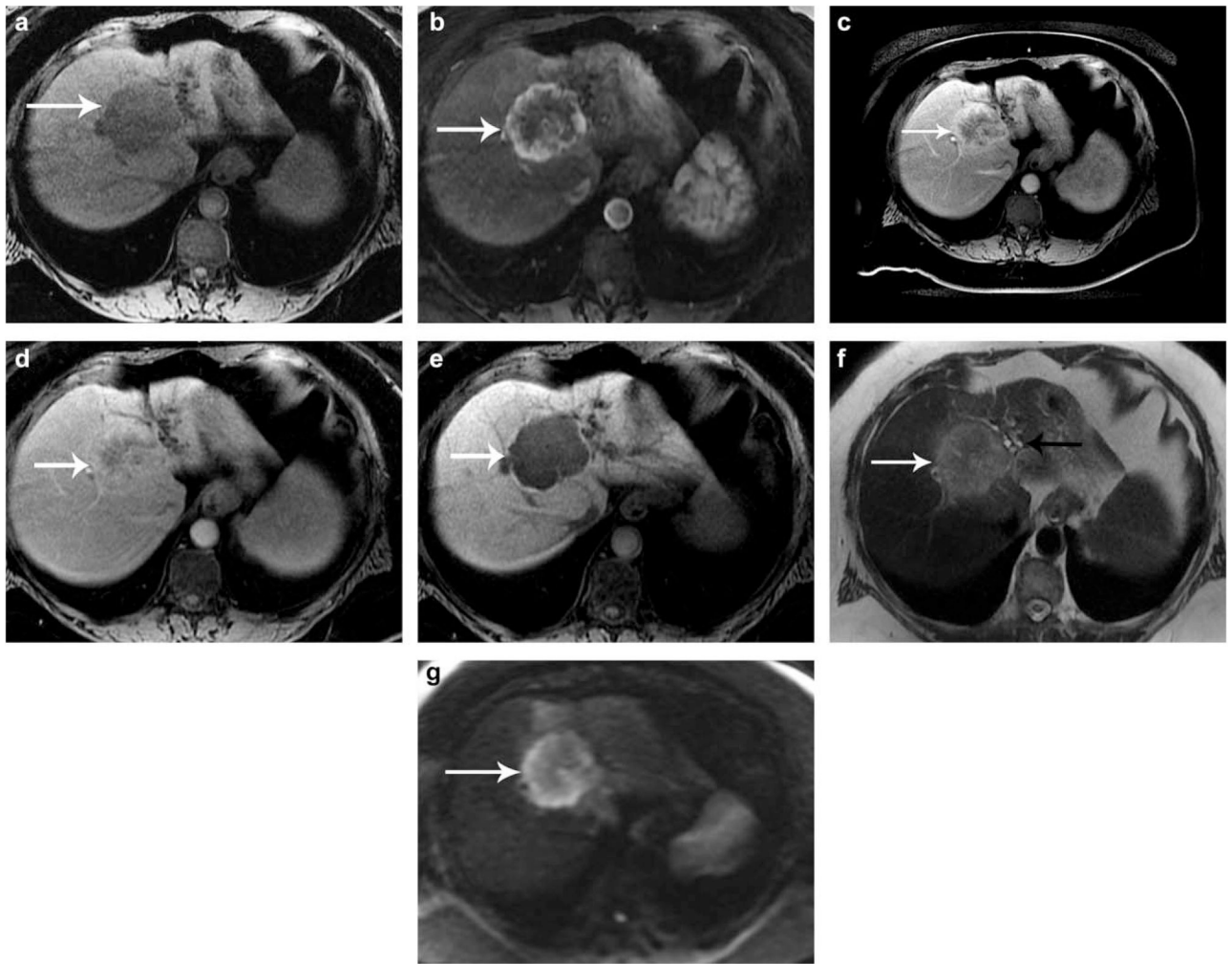


**FIGURE 4:**

A 39-year-old man with LR-M observation which was pathologically proven to represent a cholangiocarcinoma. The mass is of low signal intensity of fat-saturated T<sub>1</sub>-weighted images pregadolinium (a). This observation demonstrates rim-like enhancement on the arterial phase (b) with gradual fill-in on PVP (c) and the 5-minute delayed MRI (d) images (white arrows on each). This study was performed with gadoxetic acid, and on the 15-minute delayed images there is lack of uptake by hepatocytes in this area (e). The 5.7-cm mass demonstrates moderately high signal intensity on T<sub>2</sub>-weighted images, white arrow (f) with bile duct dilation in the atrophic left lobe (white arrow). The mass also demonstrates a rim-like high signal intensity area on diffusion-weighted images (b-800) (g).

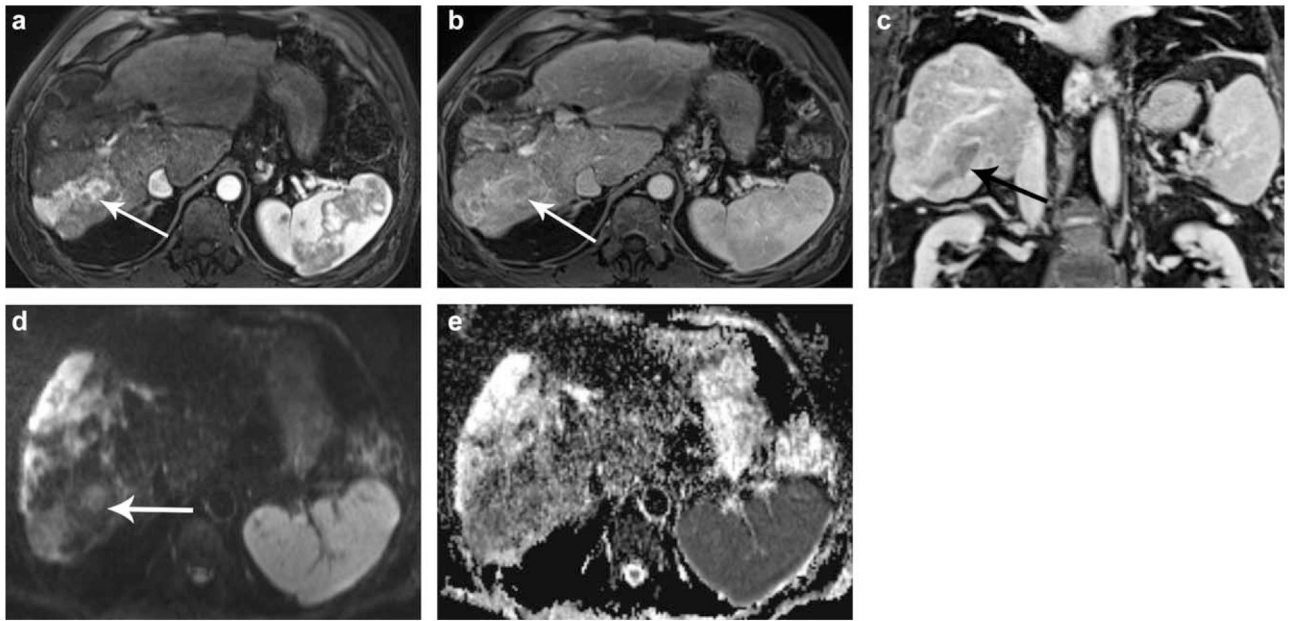


**FIGURE 5:**

A 49-year-old with hepatitis B presented with abdominal pain. Multiphase MRI demonstrates linear, arterial enhancement along the portal vein (a), which demonstrates washout on PVP (b). It is best seen as TIV on coronal PVP (c). There is some high signal intensity along the portal tract on b-800 diffusion-weighted images (d) but there is no definite restricted diffusion (e).

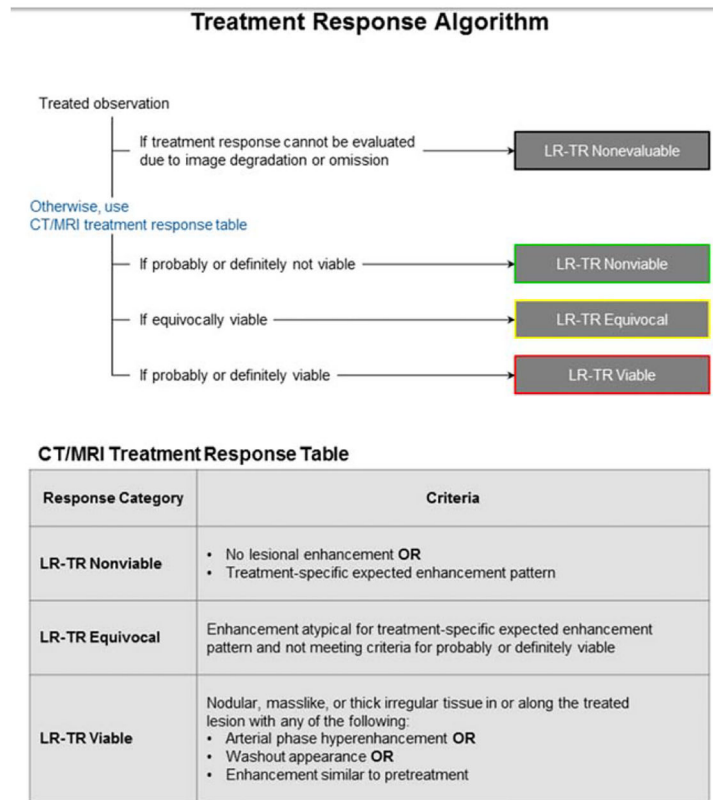


**FIGURE 6:**  
v2017 LI-RADS Treatment Response Algorithm. Reprinted with permission from the American College of Radiology.



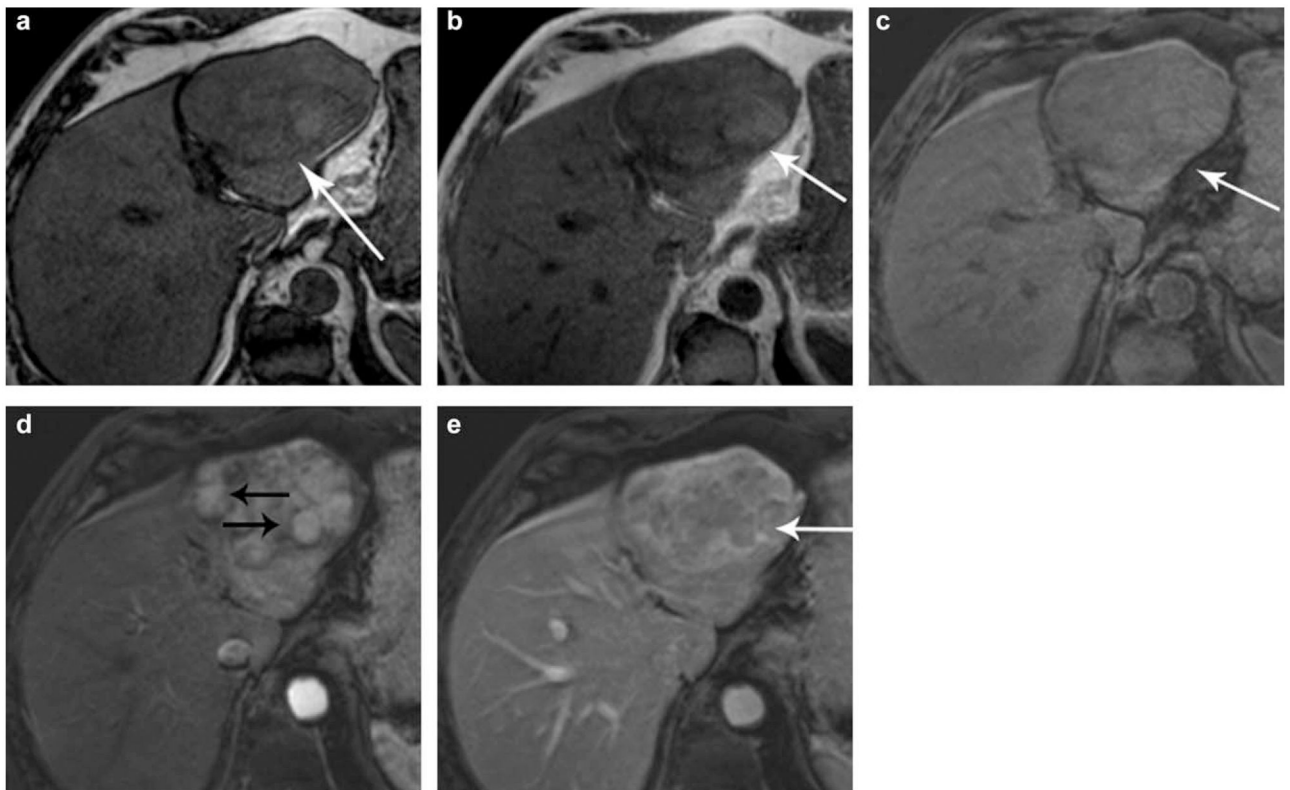


**FIGURE 7:**

HCC in a 77-year-old man with cirrhosis, (a) Axial “T<sub>1</sub>-weighted in-phase and (b) out-of-phase images show hypointense mass (white arrow), (c) Axial T<sub>1</sub>-weighted fat-saturated images obtained before and after contrast administration in (d) late arterial, (e) portal venous, and (f) delayed phase show a mass with an arterial phase hyperenhancement of a several smaller inner nodules (black arrows) within a larger nodule with washout (white arrow). This is consistent with mosaic perfusion (g). Coronal T<sub>2</sub>-weighted and (h) axial T<sub>2</sub>-weighted fat-saturated images show T<sub>2</sub> isointensity, (i–k) Axial diffusion-weighted images (b-values: 0, 400, and 800 sec/mm<sup>2</sup>, respectively) and (l) ADC map. Pathology of hepatectomy confirmed HCC.

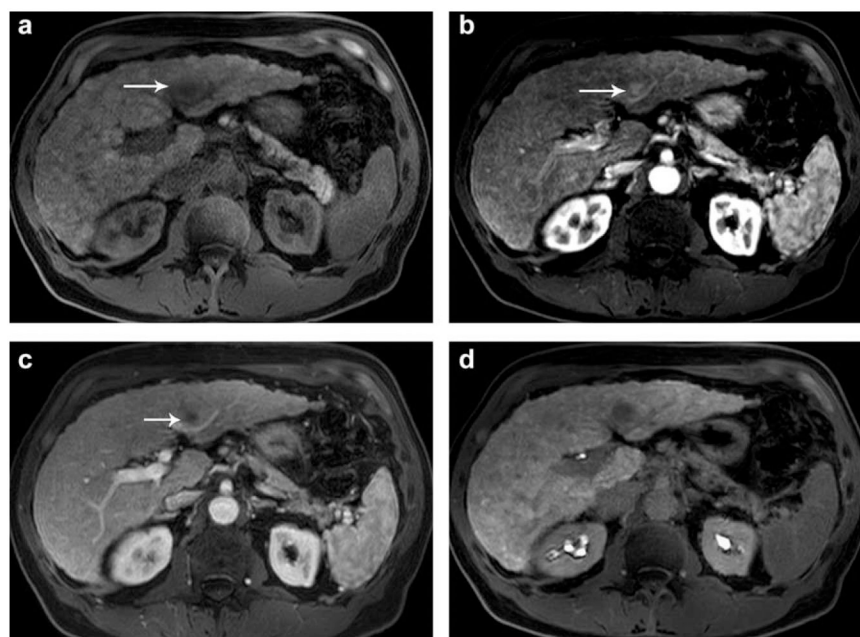


**FIGURE 8:**

Example of nodule-in-nodule appearance in a 48-year-old patient with chronic cirrhosis from hepatitis C. There is an area within this nodule which is enhancing on arterial phase (b) (arrow), but it is smaller than the overall size of the observation including in pregadolinium images (a), on the PVP (c) and on 20-minute delayed images after administration of gadoxetic acid.

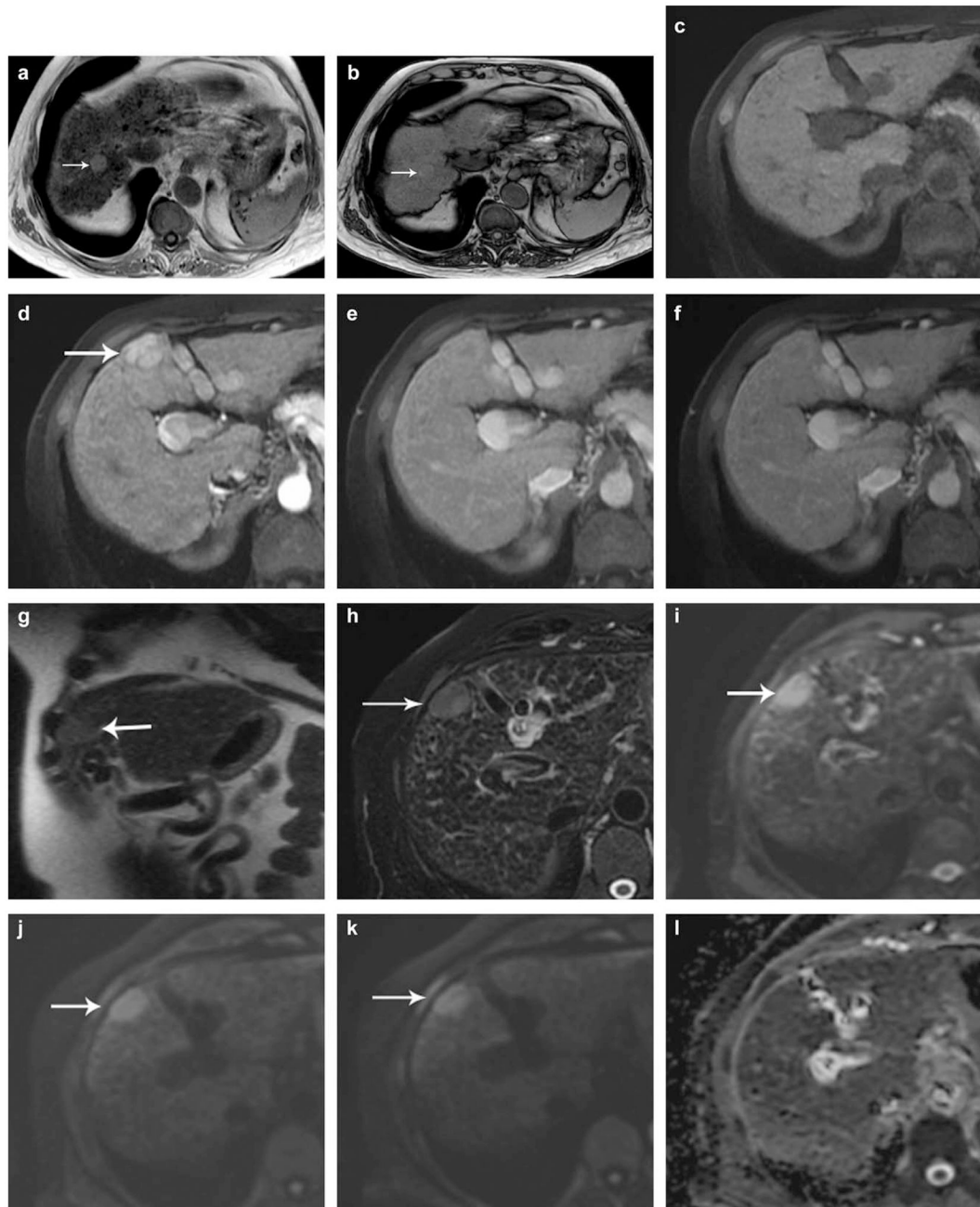


**FIGURE 9:**

Iron sparing in an observation HCC in a 54-year-old woman with primary biliary cirrhosis, (a) Axial T<sub>1</sub>-weighted in-phase and (b) out-of-phase images show iron sparing in a solid mass (arrowhead), in contrast to the signal drop observed in the background liver on the in-phase sequence (acquired with a longer echo time), (c) Axial T<sub>1</sub>-weighted fat-saturated images obtained before and after contrast administration in (d) late arterial, (e) portal venous, and (f) delayed phase show arterial hyperenhancement with washout (arrow), (g) Coronal T<sub>2</sub>-weighted and (h) axial T<sub>2</sub>-weighted fat-saturated images show mild-moderate T<sub>2</sub>

hyperintensity. (i–k) Axial diffusion-weighted images (b-values: 0, 400, and 800 sec/mm<sup>2</sup>, respectively) and (l) ADC map. Pathology of liver specimen confirmed HCC.

Author Manuscript

Author Manuscript

Author Manuscript

Author Manuscript

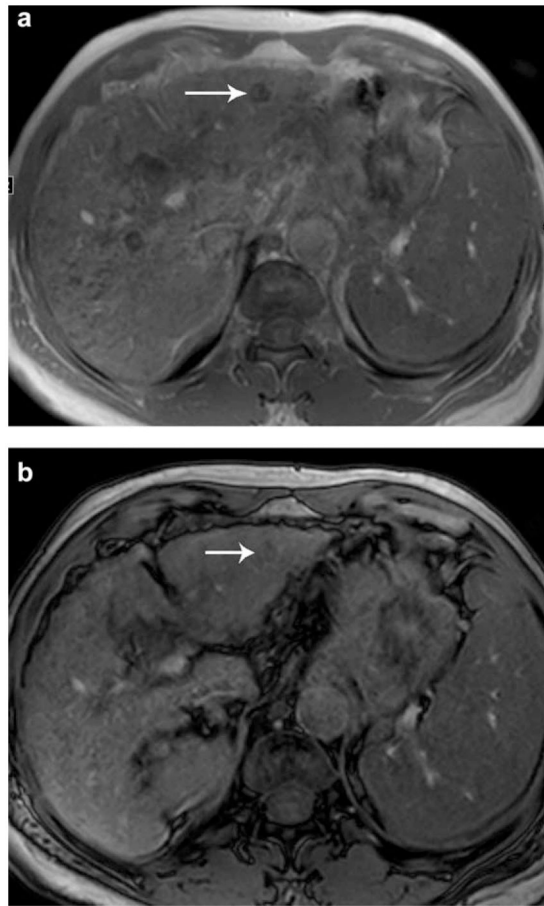


**FIGURE 10:**

Iron deposition in an observation. A 58-year-old man with known ethanol-induced cirrhosis. In segment 2 of the liver there is a 10-mm observation which is of low signal intensity on in-phase T<sub>1</sub>-weighted images and becomes somewhat higher in signal intensity on opposed-phase images (arrow). This is an example of iron deposition within an observation and represents an ancillary feature which is an ancillary feature favoring benignity. Using this ancillary feature, one could decrease the final LI-RADS category by one (so long as no other ancillary features favoring malignancy or HCC in particular were identified to negate this particular ancillary feature).

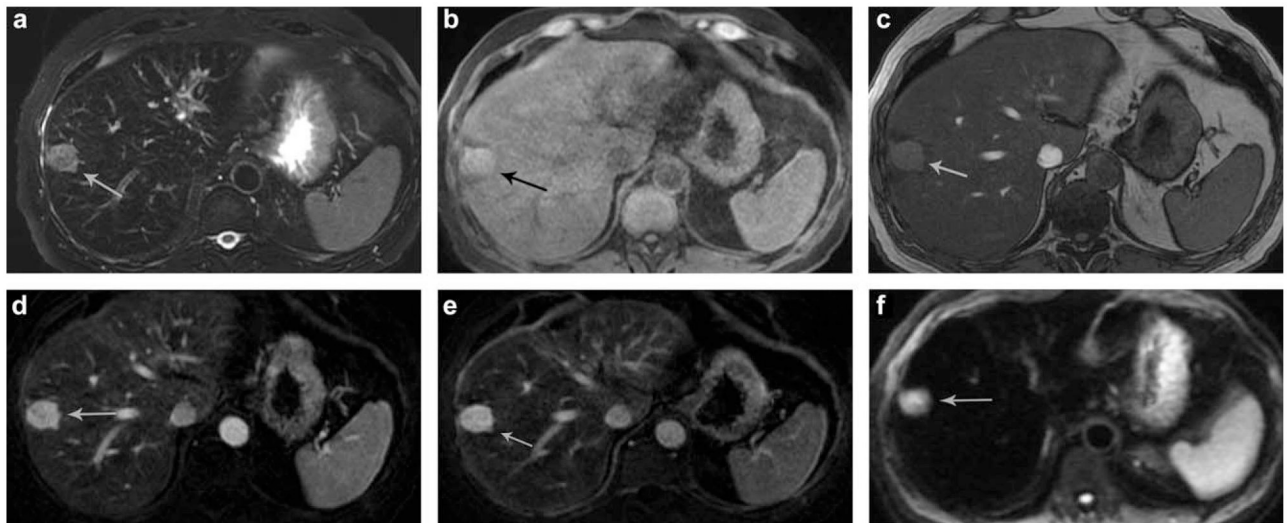


**FIGURE 11:**

Blood product in an observation. A 51-year-old man with high signal intensity observation in segment 7 of the liver and no prior for comparison. Due to the high signal intensity of the 26-mm observation on fat-saturated T<sub>1</sub>-weighted images (b), which was felt to represent blood product in a mass (ancillary feature of HCC specifically), as well as general fatty liver infiltration with low signal intensity throughout the liver parenchyma on T<sub>1</sub>-weighted, opposed-phase images (c), it can be difficult to determine if there is actual enhancement. This case illustrates utility of subtraction images (d). No washout was identified on PVP, nor on (e) the 3–5 min delayed images, although again, use of subtraction images would be helpful to review, (f) On the diffusion weighted image (b=400), there is high signal intensity in the observation. This case also illustrates moderately high signal intensity on T<sub>2</sub>-weighted images (a), which is an ancillary feature of malignancy. This was called a LI-RADS-4 observation (arterial enhancement, size >10 mm, and at least one ancillary features of malignancy). Despite there being more than one ancillary feature suggesting malignancy (moderate T<sub>2</sub> hyperintensity, blood product in the observation and restricted diffusion on ACD map; not shown), the final category cannot be upgraded higher than LI-RAD-4 without additional “major features.” This was nevertheless a pathologically proven HCC.



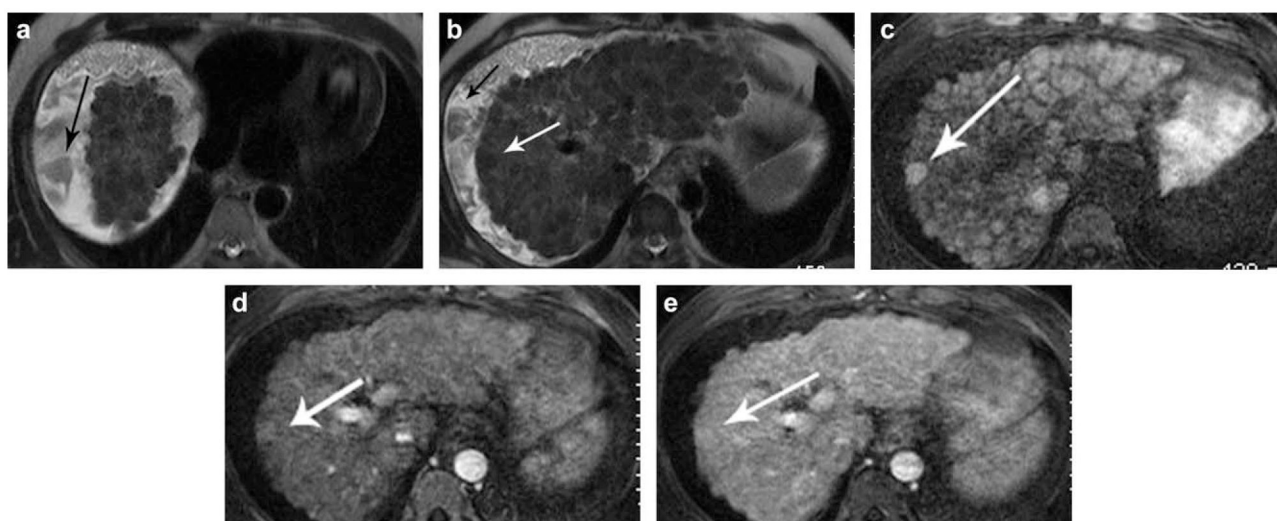


**FIGURE 12:**

Flow artifact. Example of flow artifact in ascites in a 66-year-old male patient with advanced cirrhosis from ethanol abuse, (a) Single shot fast spin-echo T<sub>2</sub>-weighted image demonstrates the presence of ascites and motion artifact of the fluid (arrow). In addition, there is a distinct 11-mm observation in segment 7 of the liver, which is of high signal intensity on T<sub>1</sub>-weighted images (b). On subtraction images, there is subtle but real-appearing arterial enhancement (c). The observation is of low signal intensity on T<sub>2</sub>-weighted images, which is not an ancillary feature at this time (e). There was no washout identified on this study nor was there a capsule. This was categorized as LI-RADS-3.



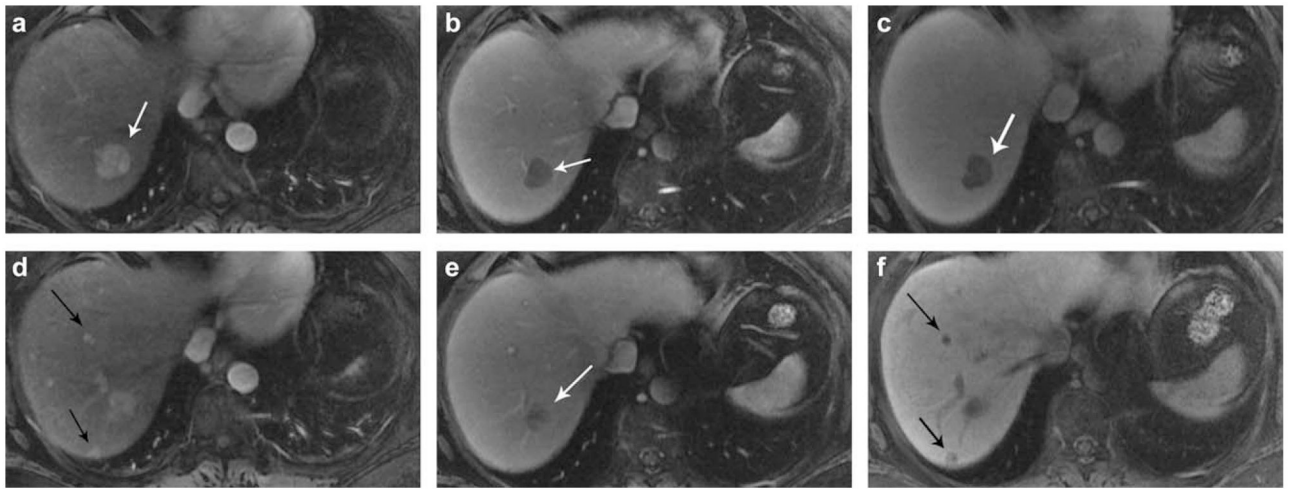


**FIGURE 13:**

Additional observations on gadoxetic acid. A 37-year-old with hepatitis B infection demonstrates presence of a 13-mm sonographically visible, arterially enhancing observation in segment 7 (a) which demonstrates washout (b) and a lack of uptake of the hepatobiliary contrast agent on the hepatobiliary phase (c) (white arrows). This is consistent with LI-RADS-5 observation. On the 20-minute delayed hepatobiliary images, two additional (d), subcentimeter observations are seen (black arrows) which also demonstrate arterial enhancement (e) but no washout on the PVP (f).



**FIGURE 14:**

A 72-year-old man undergoing TACE for previously two biopsy-proven HCCs. Both of these biopsy-proven HCC initially were a bit atypical in that they showed arterial enhancement and growth, but no washout (images not shown). At the time of TACE of the larger HCC in segment 7, Lipiodol is seen being taken up by the mass during the fluoroscopic procedure (a). An unenhanced CT scan performed with 1 month post-TACE demonstrates some high density Lipiodol in both HCCs, both in segment 7 (larger one) (b) and segment 6 (smaller one) (c) but the distribution of Lipiodol is not homogeneous. An MRI performed 3 months post-TACE images of the larger mass in segment 7 demonstrates high signal intensity on T<sub>1</sub>-weighted fat-saturated images, prior to gadolinium administration, consistent with blood products (d). On arterial phase images (e) including subtraction images (f), a few nodular areas are identified with the treated mass in segment 7 and along the periphery, which have the same imaging characteristics as pretreatment (arterial enhancement but no PVP washout (g)). Despite the lack of “washout,” these areas of enhancement are consistent with viable disease since the imaging characteristics are the same as the pretreatment characteristics. In the smaller treated lesion in segment 6, on arterial (h) (black arrow) and PVP imaging (i) (black arrow) there was no nodular enhancement and this was called nonviable. This was confirmed on subsequent MRI follow-up at 6 and 9 months after TACE.

**TABLE 1.**  
Ancillary Features Described That Are Consistent With Malignancy and Specific for HCC

Ancillary features favoring Malignancy	
Malignancy in general, not HCC in particular	HCC in particular
US visibility as discrete nodule Subthreshold growth Restricted diffusion Mild-moderate T2 hyperintensity Corona enhancement Fat sparing in solid mass Iron sparing in solid mass Transitional phase hypointensity Hepatobiliary phase hypointensity	Nonenhancing “capsule” Nodule-in-nodule Mosaic architecture Blood products in mass Fat in mass, more than adjacent liver
Ancillary features favoring Benignity	
Size stability 2 yrs Size reduction Parallels blood pool enhancement Undistorted vessels Iron in mass, more than liver Marked T2 hyperintensity Hepatobiliary phase isointensity	

Reprinted with permission.